

## A comparative study of two meta-heuristic algorithms in optimizing cost of reinforced concrete segmental lining

S.S. Mousavi, M. Nikkhah\* and Sh. Zare

Faculty of Mining, Petroleum & Geophysics Engineering, Shahrood University of Technology, Shahrood, Iran

Received 12 June 2018; received in revised form 26 October 2018; accepted 5 November 2018

### Keywords

Meta-Heuristic  
Optimization

Segmental Lining

Particle Swarm  
Optimization

Imperialist Competitive  
Algorithm

Tunnel Boring Machine

### Abstract

In this work, we tried to automatically optimize the cost of the concrete segmental lining used as a support system in the case study of Mashhad Urban Railway Line 2 located in NE Iran. Two meta-heuristic optimization methods including particle swarm optimization (PSO) and imperialist competitive algorithm (ICA) were presented. The penalty function was used for unfeasible solutions, and the segmental lining structure was defined by nine design variables: the geometrical parameters of the lining cross-section, the reinforced feature parameters, and the dowel feature parameters used among the joints to connect the segment pieces. Furthermore, the design constrains were implemented in accordance with the American Concrete Institute code (ACI318M-08) and guidelines of lining design proposed by the International Tunnel Association (ITA). The objective function consisted of the total cost of structure preparation and implementation. Consequently, the optimum design of the system was analyzed using the PSO and ICA algorithms. The results obtained showed that the objective function of the support system by the PSO and ICA algorithms reduced 12.6% and 14% per meter, respectively.

### 1. Introduction

Reinforced concrete structures have a considerable compressive strength compared to most materials. In addition to the high compressive strength, the reinforced concrete structures are durable and versatile with a relatively low maintenance cost compared with the steel structures [1]. Material cost is an important issue in the design and construction of reinforced concrete structures. The main influential factor involved in this process is the amount of the required concrete and steel reinforcement. Therefore, it is advantageous to make the concrete structures lighter, while maintaining the service ability and strength requirements. Some other significant factors involved in this regard are labour and formwork costs. Engineers must be able to design cost-efficient structures without compromising the function or violating the structural constraints.

The long-established approach to design reinforced concrete members does not fully optimize the use of materials. Most designs are based upon the prior experience of the engineers who select the cross-section dimensions and material grades correspondingly, thereby creating fixed rules-of-thumb for preliminary designs. Typically, this process is time-consuming and requires ample human efforts and material usage. The structural optimization procedures by artificial intelligence are an evident alternative to the experimental designs.

The design optimization of reinforced concrete (RC) structures is challenging due to the complexity associated with the reinforcement design. Moreover, in the case of concrete structures, three cost components must be considered due to concrete, steel, and formwork, and any variation in the quantity of each

\* Corresponding author: [m.nikkhah@shahroodut.ac.ir](mailto:m.nikkhah@shahroodut.ac.ir) (M. Nikkhah).

mentioned item affects the overall cost of the structure to a great extent. As such, selecting appropriate values for the design variables and quantity of reinforcement to minimize the total cost component is a major issue.

In a study, Kaveh and Sabzi (2011) have assessed the optimum design of reinforced concrete frames using two methods: heuristic big bang-big crunch (HBB-BC), which is based upon the big bang-big crunch (BB-BC) and a harmony search (HS) scheme to manage the variable constraint, and the HPSACO algorithm, which is a combination of particle swarm with passive congregation (PSOPC), ant colony optimization (ACO), and HS algorithms [2]. Akin and Saka (2010) have investigated the optimum detailed design of reinforced concrete continuous beams using the HS algorithm [3]. In another research work, Camp et al. (2003) have evaluated the flexural design of reinforced concrete frames using a genetic algorithm [4]. Carbonell and Gonzalez-Vidosa (2011) have studied the optimum design of reinforced concrete road vaults using the multi-start global best descent local search (MGB), meta-simulated annealing (SA), and meta-threshold acceptance (TA) [5]. Kaveh and Ilchi Ghazaan (2017) have used a harmony search-based mechanism to handle the side constraints. They combined that with the particle swarm optimization and an aging leader and challengers (ALC-PSO), resulting in a new algorithm called HALC-PSO. These two algorithms have been employed to optimize different types of skeletal structures with continuous and discrete variables [6]. Kashania et al. have utilized ICA for locating the critical failure surface and computing the factor of safety (FOS) in a slope stability analysis based on the limit equilibrium approach. They demonstrated that the proposed techniques could

provide reliable, accurate, and efficient solutions for locating the critical failure surface and relating FOS [7]. Koopialipoor et al. [8] have performed a work to evaluate/predict flyrock induced by blasting through applying three hybrid intelligent systems, namely imperialist competitive algorithm (ICA)-artificial neural network (ANN), genetic algorithm (GA)-ANN, and particle swarm optimization (PSO)-ANN.

In the current paper, the simulation algorithm of segmental lining structure was established based on the analytical solution proposed by Lee et al. (2001). Additionally, the model was combined with the two methods of particle swarm optimization (PSO) and imperialist competitive algorithm (ICA) in order to determine the optimum design variables of segmental lining in terms of constrains. In the simulation model, we also calculated the internal forces including the bending moment, axial forces, and shear forces, and in the optimization model, the optimum combination of design variables in terms of constrains were studied using PSO and ICA.

Mashhad Urban Railway Line 2 is the second metro line used to facilitate passenger transport in the city of Mashhad (Iran). The total length of the metro line 2 is approximately 14.3 km. The segment of the tunnel that runs from station C2 through L2 and further to the tunnel boring machine (TBM) exit shaft is to be constructed by mechanized tunnelling methods using TBM [9]. The current work aimed to consider the assessment of the imposed load and optimization of the segmental lining for the critical cross-section of the tunnel. Tables 1 and 2 present the geo-mechanical properties of the soil and mechanical properties of the segmental lining, respectively.

**Table 1. Geo-mechanical properties of soil [9].**

Layer Number	Layer Substance	Density (kN/m <sup>3</sup> )	Cohesion (kg/cm <sup>2</sup> )	Friction angle (Degree)	Elastic modulus (kg/cm <sup>2</sup> )
I	SC-SM	18	0	35	800
II	CL-ML	16.5	0.8	23	150
III	SC-SM	19	0	36	1000
IV	CL-ML	17	0.95	25	180
V	SC-SM	17.5	0	35	1000

**Table 2. Properties of segmental lining [10].**

Density (Kg/m <sup>3</sup> )	Internal radius (m)	Thickness (m)	Elastic modulus (GPa)
2400	4.2	0.35	35

## 2. Definition of optimization problem

### 2.1. Problem definition

Optimization is performed in order to attain the most efficient adequate segmental lining pattern with a minimum cost. The term “adequate” implies that the lining must have sufficient strength and deformation characteristics as well as the ability to meet the constraints in the formulation of the optimization function. Another objective of the optimization process is to minimize the costs of segmental lining, while guaranteeing the strength and serviceability of the ACI318-08 code and guidelines of the segmental lining design (ITA-2000) [11]. Therefore, the mathematical formulation of the objective function and optimum constraints are stated as follow:

$$\begin{aligned} F(X_1, X_2, X_3, \dots, X_n) \\ = C_C * (V_{it} - V_{is}) + C_s \\ * (V_{is} * \gamma_{is}) + C_f * A_{fb} \\ + C_b * (V_{ib} * \gamma_{ib}) \end{aligned} \quad (1)$$

$$\text{subject to } C < 0 \text{ where } C = \sum_{i=1}^n c_i \quad (2)$$

Note that  $x_1, x_2, \dots, x_n$  are the design variables for the analysis described in Section 2.2. Other necessary data for the calculation of the RC segmental lining are the parameters of the problem, as described in Section 2.3. In Eq. (1), the objective function  $F$  is the cost function, where  $V_{it}$ ,  $V_{is}$ , and  $V_{ib}$  represent the measurements of construction units (i.e. concrete, steel, and formwork), and  $C_C$ ,  $C_s$ , and  $C_b$  denote the unit prices, which are defined in accordance with the price list of road issued by the Ministry of Transportation (Iran). In Eq. (2), the constraints  $c_i$  show all the ultimate limit states (ULS) that the structure must comply with as well as the geometrical and constructability constraints of the problem.

### 2.2. Design variables

In the RC segmental lining, the design variables describe the cross-sectional characteristics and reinforcement arrangements including the bar reinforcement, stirrup reinforcement, and bolt reinforcement parameters. In the current paper, we considered nine design variables,

as follow:

1. Lining width;
2. Lining thickness;
3. Number of continuous lower reinforcements;
4. Diameters of continuous lower reinforcements;
5. Number of continuous upper reinforcements;
6. Diameters of continuous upper reinforcements;
7. Diameters of stirrups;
8. Diameters of bolts;
9. Number of the bolts used to connect the lining pieces.

Figure 1 shows the transverse and bar reinforcement variables considered in the present work.

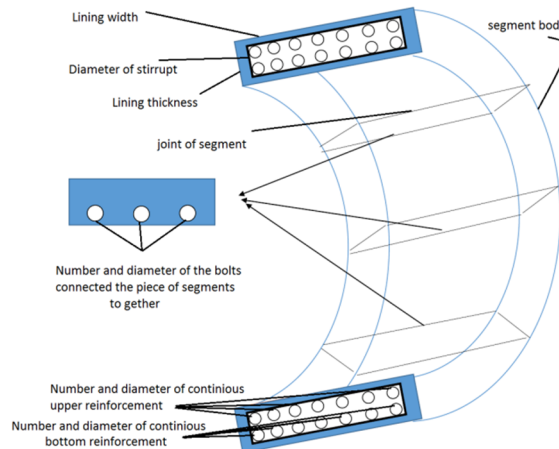
An algorithm was used to analyze the design variable limits and the corresponding step sizes required to maintain these variables within the proper range. After setting the limits and corresponding step sizes, the number of possible values used by a design parameter could be calculated based on which, the number of possible segmental lining designs was determined. The variable limits and step sizes for the segmental linings are presented in Table 3.

With a design space, the number of the possible segmental lining pattern designs was calculated to be  $1020*10^6$  (Table 3).

### 2.3. Design parameters with a fixed value

The design parameters of the analysis include all the magnitudes that are considered as the fixed data, rather than a part of the optimization process. In addition to the geometrical values, these parameters encompass the properties of the surrounding rocks, construction circumstance, and the applied TBM. In this regard, the main geometrical parameters are the radius of segmental lining centroid and the number and position of the lining joints. Stiffness modulus of the surrounding medium is the main considered parameter of the ground. Moreover, the main considered parameter regarding the construction circumstance is the grouting pressure, which must be selected cautiously. As for the applied TBM, the main parameter is the cutter head trust, which should be prepared by shield jacks. A summary of the design parameters in the RC segmental linings is presented in Table 4.

Since the tunnel elevation is above the underground water table, the water pressure was not considered as the acting parameter in segmental lining and is not given in Table 4.

**Figure 1. Schematic view of design variables.****Table 3. Design variables of segmental lining.**

<b>Variable</b>	<b>Unit</b>	<b>Lower limits</b>	<b>Step size</b>	<b>Upper limits</b>	<b>Possible value</b>
Lining width	mm	800	10	1800	101
Lining Thickness	mm	200	10	450	26
Number of continuous lower reinforcements	-	2	1	16	15
Diameters of continuous lower reinforcements	mm	12	2	22	6
Number of continuous upper reinforcements	-	2	1	16	15
Diameters of continuous upper reinforcements	mm	12	2	22	6
Diameters of stirrups	mm	10	2	12	2
Diameters of bolts	mm	18	2	32	8
Number of bolts	mm	2	1	4	3

**Table 4. Basic parameters of geometry and actions in segmental lining.**

<b>Parameters</b>	<b>Values</b>
Radius of segmental lining centroid (m)	9.10
Overburden (m)	10.4
Ring configuration	7+1 (7+key)
Soil unit weight ( $KN/m^3$ )	17.5
Jack plate diameters (mm)	230
Soil internal friction angle (degree)	28
Soil cohesion ( $Kg/cm^2$ )	0.95
Coefficient of lateral earth pressure	0.8
Thrust force of shield jacks ( $MN/m$ )	5.6
Number of shield jacks	15
Nominal strength of concrete (MPa)	50
Allowable compressive strength of concrete (MPa)	15
Allowable compressive strength of reinforcement (MPa)	350
Allowable compressive strength of bolts (MPa)	1050
Safety factor	2
Eccentricity between center of working thrust force by one jack and segmental lining centroid (mm)	10
Space between two adjacent jacks (cm)	10
Backfill grouting pressure (KPa)	100
Number of lining joints	8
Joint flexural stiffness	0.01
Surface load magnitude ( $KN/m^2$ )	20
Allowable deformation in dynamic analysis	0.002

#### 2.4. Cost function

The cost function defined in Eq. 8 represents the objective function, where

$F(x)$  is the objective function, which denotes the total cost of the segmental lining (Iranian Rial);

$C_c$  is the cost of concrete ( $Rial/m^3$ );  
 $C_s$  is the cost of steel ( $Rial/kg$ );  
 $C_f$  is the cost of formwork ( $Rial/m^2$ );  
 $C_b$  is the cost of bolt ( $Rial/kg$ );  
 $V_{it}$  is the total volume of member ( $m^3$ );

$V_{is}$  is the volume of steel reinforcement in a member ( $m^3$ );

$V_{ib}$  is the volume of steel reinforcement (bolt) in a member ( $m^3$ );

$A_f$  is the total formwork area ( $m^2$ );

$\gamma_{is}$  is the weight per unit volume of steel ( $kg/m^3$ );

$\gamma_{ib}$  is the weight per unit volume of bolt ( $kg/m^3$ );

$C$  shows the penalty (constraint violation) function, which is the summation of all the constraint violations, and

$C_i$  is the violation function of a specific constraint. Cost function encompasses the price of materials (concrete, steel, and formwork) and all the entries required to evaluate the full cost of the segmental lining per linear meter (*Rial/m*). To assess the fitness of a trial design and determine its distance from the global optimum, the eventual constraint violation was computed using a penalty function, which consisted of a series of geometric constraints corresponding to the dimensions and shape of the cross-sections. In addition, the function had a series of constraints correlating to the construction and internal forces of the structure. As such, the penalty would be proportional to the constraint violations, and the most efficient design with the minimum cost had no penalty. The penalized objective function measures the applicability of a solution, as follows:

$$\varphi(x) = F(x) \cdot [1 + KC]^\epsilon \quad (3)$$

where  $\varphi(x)$  denotes the penalized objective function (*Rial*),  $K$  is the penalty function constant, and  $\epsilon$  shows the penalty function exponent. In the current work, the  $K$  and  $\epsilon$  values were estimated to be 1.0 and 2.0, respectively, as recommended by Kaveh & Sabzi (2011).

The constraint violation was as follows:

$$C = \sum_{i=1}^n c_i \quad (4)$$

where  $c_i$  represents the violation function of a specific constraint. In total, 18 constraints were set to obtain an adequate segmental lining in the present work. The theoretical background and calculation of the penalty function for these constraints are discussed in the following section.

## 2.5. Design constraints and provisions

The following constraints were considered for designing a segmental lining in accordance with the American Concrete Institute code (ACI318M-08) and guidelines of segmental lining design (ITA, 2000):

**1) Axial Strength:** The axial

strength of the lining ( $\phi P_n$ ) should be larger than twice the value of the applied factor load ( $P_u$ ). Therefore, the axial strength of constraint  $c_1$  is calculated as follows:

$$C_1 = \frac{P_u - \phi P_n}{\phi P_n} \geq 0 \quad (5)$$

**2) Moment:** A column should have a sufficient bending strength ( $\phi M_n$ ) in order to resist the applied bending moment ( $M_u$ ). Therefore, the flexural strength of constraint  $c_2$  was calculated as follows:

$$C_2 = \frac{M_u - \phi M_n}{\phi M_n} \geq 0 \quad (6)$$

**3) Shear Strength:** A column should have a sufficient shear strength ( $\phi V_n$ ) in order to resist the applied shear force ( $V_u$ ). Therefore, the shear strength of constraint  $c_3$  was calculated as follows:

$$C_3 = \frac{V_u - \phi V_n}{\phi V_n} \geq 0 \quad (7)$$

**4) Minimum Reinforcement Ratio:** The reinforcement ratio ( $\rho_t$ ) cannot be less than the minimum reinforcement ratio ( $\rho_{min}$ ), as proposed by ACI. Therefore, the minimum reinforcement of constraint  $c_4$  was determined as follows:

$$C_4 = \frac{\text{Max} \left\{ \frac{\frac{1.4}{f_y}}{\frac{0.25\sqrt{f_c}}{f_y}} \right\} - \rho_t}{\text{Max} \left\{ \frac{\frac{1.4}{f_y}}{\frac{0.25\sqrt{f_c}}{f_y}} \right\}} \geq 0 \quad (8)$$

**5) Maximum Reinforcement Ratio:** The reinforcement ratio ( $\rho$ ) cannot exceed 8%. Therefore,  $c_5$  could be calculated as follows:

$$C_5 = \frac{\rho - 0.08}{0.08} \geq 0 \quad (9)$$

**6) Minimum Bar Spacing:** An adequate bar spacing in segmental lining must be provided to allow the smooth flow of concrete and avoid segregation. Therefore, the minimum spacing of constraint  $c_6$  was determined as follows:

$$C_6 = \frac{\text{Max} \left\{ \frac{d_b}{25 \text{ mm}} \right\} - s}{\text{Max} \left\{ \frac{d_b}{25 \text{ mm}} \right\}} \geq 0 \quad (10)$$

**7) Minimum Reinforcement Ductility:** Failure

of the flexural members with ductility requires the strain in the extreme steel layer ( $\varepsilon_t$ ) to exceed 0.004:

$$C_7 = \frac{0.004 - \varepsilon_t}{0.004} \geq 0 \quad (11)$$

**8) Minimum Bolt Reinforcement Ratio:** The reinforcement ratio of the bolt ( $\rho_b$ ) cannot be considered less than 1% due to the two pieces of segmental lining. Moreover, the shear stresses caused by internal forces should have resistance against the shear and tension stresses caused by the jack thrusts. As such, the minimum reinforcement of constraint c8 was determined as follows:

$$C_8 = \frac{0.01 - \rho_b}{0.01} \geq 0 \quad (12)$$

**9) Maximum Bolt Reinforcement Ratio:** The reinforcement ratio ( $\rho_b$ ) cannot exceed 8%. Therefore, c9 could be calculated as follows:

$$C_9 = \frac{\rho_b - 0.08}{0.08} \geq 0 \quad (13)$$

**10) Joints:** According to the guidelines of the International Tunnel Association for segmental lining design, the moment-resisting of the joints should not be less than 60% of the segmental lining resisting moment. Therefore, this constrain was considered as follows:

$$C_{10} = \frac{(0.6 * M_{lining}) - M_{joint}}{M_{joint}} \geq 0 \quad (14)$$

where  $M_{lining}$  represents the moment-resisting of the segmental lining and  $M_{joint}$  is the moment-resisting of the lining joints.

**11) Shear Resistance of Bolts against Imposed Shear Forces:** In the segmental lining joints, the

bolts must have resistance against the shear forces imposed by medium external pressures, TBM jack thrust pressures, and backfill grouting pressure. In the following section, the violation functions regarding these imposed shear stresses have been expressed in Eqs. (15 and 16), respectively.

$$C_{11} = \frac{V_u - V_{bolt}}{V_{bolt}} \geq 0 \quad (15)$$

$$C_{12} = \frac{V_{jacks} - V_{bolt}}{V_{bolt}} \geq 0 \quad (16)$$

$$C_{13} = \frac{V_{grouting} - V_{bolt}}{V_{bolt}} \geq 0 \quad (17)$$

**12) Segmental Strength against Jack Pressures:** According to the guidelines of ACI (2000), the segmental body must have enough strength to resist the pressure caused by jack thrusts in order to avoid crack appearance and growth. Therefore, the amount of imposed pressure by the jacks ( $\sigma_{jacks}$ ) should not exceed the nominal compressive strength of concrete ( $\sigma_{ca}$ ) [11]. Mathematically, this constrain is expressed as follows:

$$C_{14} = \frac{\sigma_{jacks} - \sigma_{ca}}{\sigma_{ca}} \geq 0 \quad (18)$$

**13) Resistance against Earthquake:** In this constrain, the effects of design earthquake for the dynamic stability of the segmental lining have been discussed. In order to analyze dynamic stability, the soil-structure interaction approach was utilized using the analytical equation under no-slip and full-slip conditions, as proposed by Wang and Penzien in 1993 and 2000, respectively [12, 13]. The analytical equations and their parameters are presented in Tables 5 and 6, respectively.

Table 5. Equations used for dynamic analysis [10, 11].

Full-slip	No-slip	Method
$T_{max} = \pm \frac{1}{6} K_1 \frac{E_m r \gamma_{max}}{(1 + \nu_m)}$	$T_{max} = \pm K_2 \frac{E_m r \gamma_{max}}{2(1 + \nu_m)}$	
$M_{max} = \pm \frac{1}{6} K_1 \frac{E_m r^2 \gamma_{max}}{(1 + \nu_m)}$	$M_{max} = \pm \frac{1}{6} K_1 \frac{E_m r^2 \gamma_{max}}{(1 + \nu_m)}$	
$F = \frac{1}{6} \frac{E_m r^3 (1 - \nu_l^2)}{E_l I (1 + \nu_m)}$	$C = \frac{E_m r (1 - \nu_l^2)}{E_l t (1 + \nu_m) (1 - 2\nu_m)}$	
$V_{max} = \pm \frac{12 E_l I R^n \gamma_{max}}{d^2 (1 - \nu_l^2)}$	$V_{max} = \pm \frac{12 E_l I R^n \gamma_{max}}{d^2 (1 - \nu_l^2)}$	
$\alpha^n = \frac{12 E_l I (5 - 6\nu_m)}{d^3 G_m (1 - \nu_l^2)}$	$\alpha = \frac{24 E_l I (3 - 4\nu_m)}{d^3 G_m (1 - \nu_l^2)}$	Penzien (2000)
$R^n = \frac{4(1 - \nu_m)}{\alpha^n + 1}$	$R = \pm \frac{4(1 - \nu_m)}{\alpha + 1}$	

**Table 6. Definition of parameters used in dynamic analysis [12, 13].**

Parameter	Description	Parameter	Description
C	Compressibility ratio	$T_{max}$	Maximum axial force
$E_l$	Modulus of lining elasticity	$M_{max}$	Maximum bending moment
$\nu_l$	Poisson's lining ratio	$V_{max}$	Maximum shear force
F	Lining flexibility ratio	$\gamma_{max}$	Maximum free-field shear strain
t	Lining thickness	$\nu_m$	Poisson's medium ratio
I	Tunnel lining moment of inertia (per unit width)	$E_m$	Modulus of medium elasticity
r, d	Tunnel lining radius and diameters	$\Delta d$	Lining deflections

In this constrain, all the possible Wang and Penzien equations were calculated for each single-pattern design proposed by the algorithms, while the maximum shear force ( $V_{seismic}$ ), axial force ( $P_{seismic}$ ), and bending moment ( $M_{seismic}$ ) were considered as the imposed load of earthquake. Additionally, the stability of the segmental body and bolts was determined since this constrain had been prepared using four independent constrains. The mathematical expression in this regard is as follows:

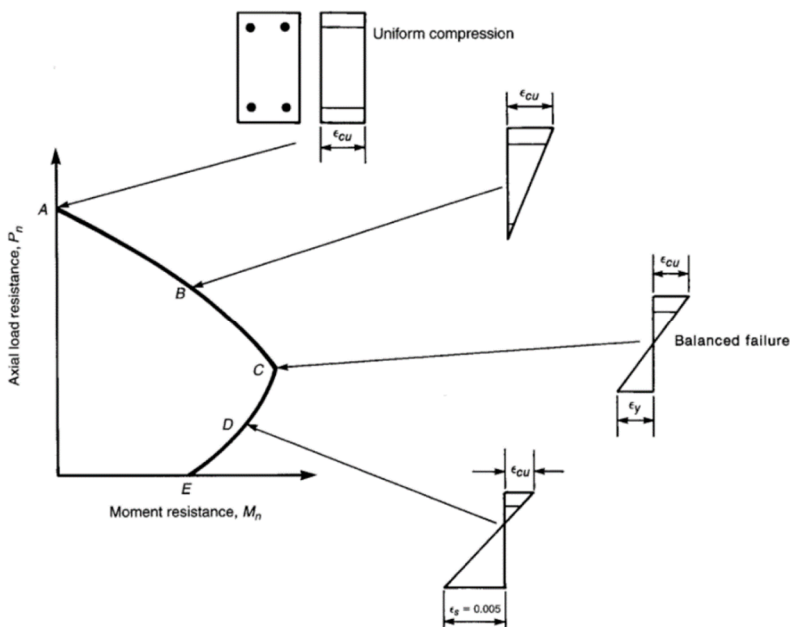
$$C_{15} = \frac{V_{seismic} - \phi V_n}{\phi V_n} \geq 0 \quad (19)$$

$$C_{16} = \frac{P_{seismic} - \phi P_n}{\phi P_n} \geq 0 \quad (20)$$

$$C_{17} = \frac{M_{seismic} - \phi M_n}{\phi M_n} \geq 0 \quad (21)$$

$$C_{18} = \frac{V_{seismic} - V_{bolt}}{V_{bolt}} \geq 0 \quad (22)$$

In the present work, the strength interaction diagrams were used to prepare the strength parameters. Segmental linings must have resistance against axial forces, bending moments, and shear forces, simultaneously. The interdependency of the axial forces and bending moment result in an interaction diagram to provide a combination of the axial forces and the bending moment, ultimately demonstrating the failure of reinforced concrete sections. This interaction diagram is depicted in Figure 2 with five characteristic points and their strain distributions [14].

**Figure 2. Nominal interaction diagram [14].**

**1) Point A-Pure Axial Load:** In Figure 2, point A and its corresponding strain distribution represent the uniform axial compression without a moment, which is considered as the largest nominal axial load for the column to support.

**2) Point B-Zero Tension, Onset of Cracking:**

The strain distribution at B in Figure 2 corresponds to the axial load and moment at the onset of concrete crack as the concrete strains on the opposite face of the column reach zero. Case B demonstrates the onset of cracking in the least compressed side of the column. Since the tensile

stresses are neglected in strength calculations, the failure loads below point B in the interaction diagram represent the cases where the section is partially cracked.

### 3) Region A-C-Compression Controlled Failures:

Initial failure could be observed in the column with the axial load  $P_u$  and moment  $M_u$ , which falls on the upper branch of the interaction diagram between points A and C. This was attributed to the crushing of the compression face before the yielding of the reinforcement's extreme tensile layer; therefore, they are known as the compression controlled columns.

### 4) Point C-Balanced Failure, Compression Controlled Limit Strain:

In Figure 2, point C corresponds to a strain distribution with a maximum compressive strain of 0.003 on one face of the section and tensile strain, which is equal to the yield strain in the farthest layer of the reinforcement from the column's compression face.

**5) Point D-Tensile Controlled Limit:** In Figure 2, point D corresponds to a strain distribution with the compressive strain of 0.003 on the top face as well as the tensile strain of 0.005 in the extreme layer of the tension steel. Failure of this column would be ductile along with the crashing of the steel strains, which is approximately 2.5 times the yield strain for 420 MPa reinforcement. Therefore, the strain of 0.005 was selected to be significantly higher compared to the yielding strain in order to ensure ductile failure.

**6) Region C-D-Transition Region:** Flexural members and columns with loads and moments that would plot between the points C and D in Figure 2 are known as transition failures since the magnitude of the curvatures at the critical section is in a transition between the ultimate curvature corresponding to the steel strains of 0.002 and 0.005. This is reflected in the transition of the strength reduction factor from 0.65 to 0.9 in the rectangular tied columns.

## 3. Applied metaheuristic algorithms

A metaheuristic technique seeks near-optimal solutions at a reasonable computational cost without the ability to guarantee feasibility or optimality. Typically, metaheuristic methods are far less time-consuming compared to the exact techniques. Heuristics could be constructive (building a solution piece by piece) or improvement-based (altering a solution to find a better one) [14].

The metaheuristic optimization methods used in the present work include the variants of the

descent local search with the most efficient global strategy, particle swarm optimization, and imperialist competitive algorithm optimization process, which starts with one initial solution and is improved iteratively. In this regard, a specific mechanism is required for moving from one solution to a closer one within the neighborhood as well as a certain acceptance criterion for the new solutions. The neighborhood of a solution is defined as the set of solutions that can be obtained through slight modifications of the current solution.

### 3.1. Particle swarm optimization (PSO)

The PSO algorithms are nature-inspired population-based metaheuristic algorithms that are originally accredited to Kennedy and Eberhart, (1995) [15]. PSO algorithms mimic the social behaviors in bird flocking and fish schooling. Starting from a randomly distributed set of particles (i.e. potential solutions), PSO algorithms are applied in order to improve the solutions based on a quality measure (i.e. fitness function). The improvisation is performed through moving the particles around the search space using a set of simple mathematical expressions, which model interparticle communications. In their simplest and most basic form, these mathematical expressions suggest the movement of each particle toward its best experienced position as well as the best position of the swarm along with random perturbations [16].

There is an abundance of different variants using different updating rules. The earliest attempt to apply this concept in simulating social behaviors was made by Kennedy and Eberhart, which resulted in a set of agents randomly spread over a torus pixel grid by adopting two main strategies: nearest neighbor velocity matching and craziness. At each iteration, a loop was determined in the program for each agent, with the other agent considered as its nearest neighbor. Following that, the velocities of the two agents X and Y were assigned to the agent in focus. As predicted, it was observed that the sole use of the strategy would quickly settle down the swarm in a unanimous, unchanging direction. In order to avoid this, we introduced a stochastic variable, known as craziness. At each iteration, some changes were applied to the velocities of the randomly selected X and Y agents, which resulted in sufficient variations into the system in order to render the simulation more "life-like" in appearance [15, 17]. Considering the mentioned observations, it could be inferred that one of the most essential features

of PSO to indicate its seemingly unalterable, non-deterministic nature is the incorporation of randomness. As a further step in this regard, Kennedy and Eberhart replaced the notion of "roost" (a place recognized by birds) in the theory proposed by Heppner and Grenander with "food" (for which the birds must search). As a result, they converted the social simulation algorithm into an optimization paradigm. The idea was to let the agents (birds) find an unknown favorable place in the search space (food source) through capitalizing on each other's knowledge. Each agent was able to remember the best position for itself and the entire swarm. The extremum of the mathematical function to be optimized could be considered as the food source. The rules for calculating the next position of a particle were introduced as follows [16, 17]:

$$v_{i,j}^{k+1} = v_{i,j}^k + c_1 r_1 (x_{best_{i,j}}^k - x_{i,j}^k) + c_2 r_2 (x_{gbest_j}^k - x_{i,j}^k) \quad (23)$$

$$x_{i,j}^{k+1} = x_{i,j}^k + v_{i,j}^{k+1} \quad (24)$$

where  $x_{i,j}^k$  and  $v_{i,j}^k$  are the jth components of the ith particle's position and velocity vector, respectively, in the kth iteration,  $r_1$  and  $r_2$  represent two random numbers uniformly distributed in the range (1,0),  $x_{best_i}$  and  $x_{gbest}$  denote the best positions experienced so far by the ith particle and whole swarm, respectively, and  $c_1$  and  $c_2$  are two parameters representing the particle's confidence in itself (cognition) and the swarm (social behavior), respectively [17].

A schematic movement of a particle is illustrated in Figure 3.

In PSO, the potential results, titled as particles, hover through the problem space by following the present optimal particles. The advantages of PSO are that PSO is easy to implement and there are few parameters to set [18].

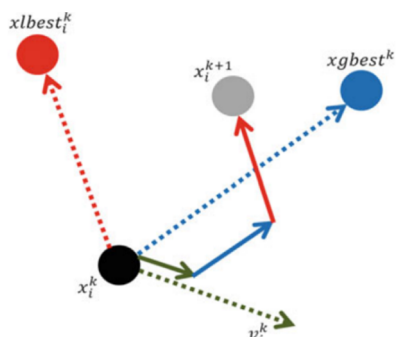


**Figure 3. Schematic movement of a particle in PSO [17].**

### 3.2. Imperialist Competitive Algorithm (ICA)

ICA has been proposed by Atashpaz-Gargari and Lucas (2007) as a new global heuristic search method, which applies the imperialism and imperialistic competition processes as a source of inspiration [18]. The beginning of ICA is with a production of randomly initial population called countries. The pseudo-code of ICA steps is demonstrated as follows:

- Choose some random points on the functions and start the empires.
- Precede the colonies toward their relevant imperialist.
- If there is a colony in an empire with lower cost than that of imperialist, swap the position of that colony and the imperialist.
- Calculate the total cost of all empires (related to the power of both imperialist and its colonies).
- Select the weakest colony (colonies) from the weakest empire and give it (them) to the empire with the most likelihood to possess it (imperialistic competition).
- Omit the powerless empires.
- If there is just one empire, stop, else go to step 2.

ICA starts with an initial population; some of the best individuals of the population (i.e. countries) are selected as the imperialist states, while the remaining account for the colonies of these imperialists. Due to the powers of the imperialists that are reversely proportional to their cost, the colonies of initial population are divided among them. Having distributed the colonies among imperialists and establishing the initial empires, these colonies commence proceeding toward their relevant imperialist country. Figure 4 depicts the movement of a colony toward the imperialist in ICA. In this movement, h and x are arbitrary numbers, which are generated uniformly as  $x \sim U(0, b*d)$  and  $h \sim U(-\gamma, \gamma)$ . Moreover, d is the distance between the colony and imperialist, and b must be greater than one. As a result of this constraint, the colonies get closer to the imperialist state from both sides [18, 19].

Additionally,  $\gamma$  is a parameter that adopts the deviation from the main direction. Although b and  $\gamma$  are random numbers, their fitting values are estimated at approximately 2 and  $\pi/4$  (radian), respectively, most of the time. More explicitly, a percentage of the mean power of each imperialist's colonies is added to power of imperialist to form the total power of an empire. Any empire that does not improve in imperialist competition will be diminished. As a result, the

imperialistic competition will grow the power of great empires and weaken the frail ones. Hence, weak empires will collapse finally. The movement of colonies toward their related imperialists along with competition among empires and also collapse mechanism will bring out the countries to converge to a state in which there exists just one empire in the world, and all the rests are its colonies. In the final stage, the colonies have the same position and power as the imperialist [19].

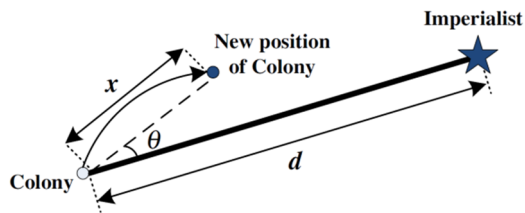


**Figure 4. Movement of colonies toward their imperialist [19].**

#### 4. Application of Algorithms

In general, preparation of an optimal design model of segmental lining requires a combination of simulation and optimization algorithms in an iterative process. Segmental lining simulation model analyzes the behavior of structures based on the design variables, which must be defined at the beginning of the optimization problems. In this analytical process, the accuracy of design constrains is evaluated as well.

In the present work, if all the segmental lining design constrains (see Section 3.4) were met, the resulting segmental lining plan would be considered to be a practical design pattern. On the other hand, if the total segmental lining design constrains were not satisfied, the resulting pattern would be classified as an impractical solution. With regard to this principle, there are numerous possible combinations for the segmental lining design variables as well as infinitive practical patterns so that their assessment seems unnecessary. Therefore, an optimization model could be used to reduce the number of design analyses efficiently. In the proposed combination model, the PSO and ICA algorithms were used as the optimization models; however, the mentioned procedure could not be imported to complex optimization problems since these models were normally non-linear and applied for large-scale problems. In such cases, simulation models would be combined for the optimization model through an iterative procedure to be regarded as an independent model.

In the current work, certain properties of the

design problem justified the use of a hybrid model in the metaheuristic and simulation algorithms. Furthermore, the obstacles associated with the system behavior and segmental lining design pattern must guarantee the acceptable safety factor of the system behavior against the imposed external forces. These non-linear system obstacles are completely non-convex in the decision space of the problems; as such, there are some different local optimal spots that cancel the compressive definition of mathematical optimization models based on gradient solutions. Therefore, the proposed hybrid optimization-simulation method could present the design variables near the optimum value by maintaining accuracy and precision.

If the gradient-based optimization methods are used for these problems, there will be some approximation in the simulation of the segmental lining, the results of which might decrease the precision of the segmental lining simulation, thereby significantly affecting the final result of the optimization problem. In the current research work, strength parameters for the interaction curve of the reinforced concrete lining were calculated, as presented in the following section. Afterwards, the imposed bending moment, axial forces, and shear forces were referred to the optimization model.

In the following section, by adding the violation to the problem cost function, the fitness degree of the unacceptable design patterns decreased. Moreover, the next position and other basic parameters of the algorithms (e.g. position and velocity of particles in PSO) were calculated again based on the research methodology in various types of meta-heuristic optimization algorithms. Combination process of the optimization and simulation models is illustrated in Figure 5.

In the current research work, we developed two programs by the MATLAB software for the optimal design of the segmental lining in Mashhad subway tunnels. In these programs, the first code was related to the simulation of the segmental lining behavior, and the output of the program determined the imposed internal forces. The code was written based on the analytical solutions proposed by Lee et al. (2001) [20]. The second code represented the optimization model of the PSO and ICA algorithms, in which the input data was received from the simulation algorithm and the optimal segmental lining design parameters were considered as the output data. After combining these models, the optimal design

variables of the segmental lining would be presented as the output data of these algorithms. Table 7 shows the results of the comparison between the design parameters and costs of

designing and implementing RC segmental lining for Mashhad subway tunnels by PSO and ICA, as well as the conventional design method used by the consulting company.

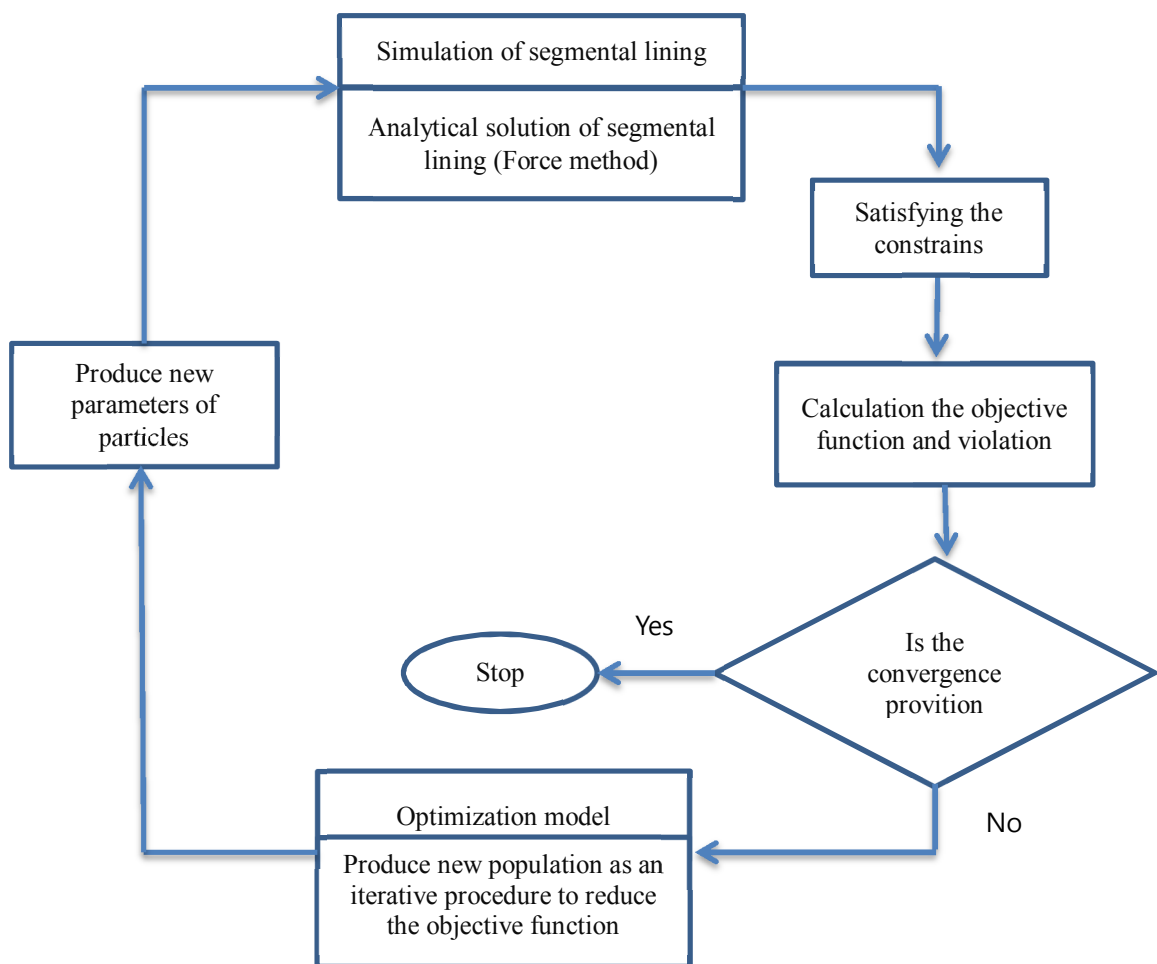


**Fig 5. Combination process of simulation and optimization algorithms.**

**Table 7. Comparison of simulation-optimization hybrid model and conventional method.**

Design variables	PSO	ICA	Conventional method of segmental lining design
Lining length (mm)	1220	1130	1500
Lining thickness (mm)	310	290	350
Number of continuous lower reinforcements	8	7	12
Diameters of continuous lower reinforcements (mm)	18	18	14
Number of continuous upper reinforcements (mm)	8	7	12
Diameters of continuous upper reinforcements (mm)	16	16	14
Diameters of stirrups mm)	10	10	12
Diameters of bolts (mm)	20	18	16
Number of bolts	3	3	2
(*) Cost of segmental lining (Rial/m)*107	4.7375	4.6827	5.4241
(*) 34000 IRR. = 1 USD			

According to the results of the hybrid model, meta-heuristic algorithms have an acceptable ability to optimize the RC segmental lining as a structural tunnel support in mechanized tunneling. Using the PSO and ICA algorithms as an optimization model, the costs of designing and implementing the RC segmental lining for Mashhad subway project were estimated at  $4.7375 \times 10^7$  and  $4.6827 \times 10^7$  Rial/m in 2015, respectively (the US dollar exchange rate to Rial is about 34000 Rial), which are 12.6% and 14% lower than the cost of the segmental lining designed based on the conventional method by the consulting company.

Convergence history of the most effectual test program for the PSO and ICA algorithms is shown in Figure 6. As it can be seen, a typical convergence history, which starts with a very steep slope and turns into a steady state afterwards, is characterized by a low slope since the program reaches near-optimal costs by making further improvement harder.

As depicted in Figure 6, convergence of the objective function in the ICA algorithm occurs at the same time as the PSO algorithm, with the minimum objective function of ICA estimated at 1.4% lower than the objective function obtained by the PSO. Therefore, it could be inferred that in these types of problems, the ICA algorithm is more applicable compared to the PSO algorithm, while the following analyses are established by the ICA algorithm as an optimization model. Mean, minimum, and cost results for 10 runs with initial random solutions are presented in Table 8. According to the information in this table, the results had a slight difference with the mean values of all the analyses; therefore, it could be concluded that the method is almost insensitive to the selection of the initial solution. As the mechanism of the optimization program method has been clarified, sensitive analysis of different geo-mechanical properties as well as the medium and different mechanical properties of the force methods equations were conducted.

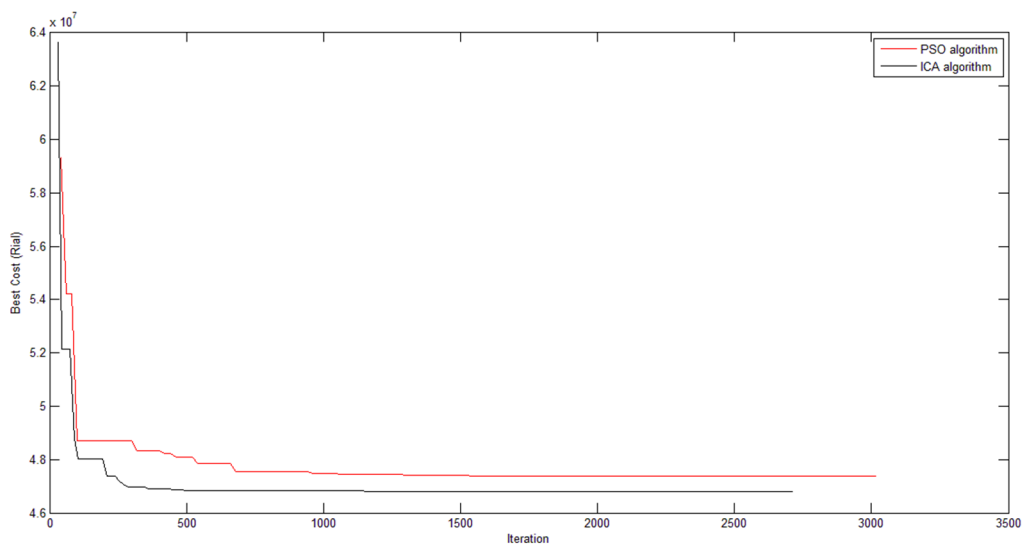


**Figure 6. Convergence history of segmental lining optimization.**

**Table 8. Cost of segmental lining pattern using PSO and ICA algorithms in 10-time program run**

Run	PSO cost (Rial/m)*107	ICA cost (Rial/m)*107
R01	4.759	4.70312
R02	4.793	4.712
R03	4.739	4.6846
R04	4.811	4.723
R05	4.7375	4.6827
R06	4.8522	4.6882
R07	4.8066	4.744
R08	4.739	4.829
R09	4.831	4.7235
R10	4.762	4.8130
Minimum	4.7375	4.6827
Mean	4.7826	4.7303

Figure 7 shows the effect of soil resistance coefficient ( $K_s$ ) on a logarithmic scale on the changes of the objective function. As mentioned earlier, increased soil resistance coefficient could enhance the rock strength specification. As such, heightening the soil resistance coefficient is associated with the decreased deformation of the segmental lining. In addition, higher soil resistance coefficient is associated with the reduction of the bending moments, while the imposed soil resistance pressure rises, thereby increasing the axial forces imposed on the segmental lining. As it can be seen in Figure 7, a higher soil resistance coefficient ( $K_s$ ) diminishes the cost of segmental lining since the reduction of the  $K_s$  coefficient leads to heightened imposed bending moment. Therefore, to satisfy constrained optimization problems against these internal forces, the load capacity of the segmental lining must increase so that the cost of segmental lining implementation per meter would rise.

Effect of joint flexural stiffness on the changes in the cost function of the problem is depicted in Figure 8. As mentioned earlier, joint flexural

stiffness and bending moment decrease in a parallel fashion. Furthermore, reduced joint flexural stiffness is associated with the higher deformation of the segments and imposed soil resistance pressure, thereby increasing the imposed internal axial forces.

As it can be seen in this figure, an increase in the joint flexural stiffness causes the lining behavior to act as a continuous structure, which, in turn, raises the imposed loading, leading to the subsequent increase in the costs of lining design and implementation.

Effect of number of lining joints on the cost function is depicted in Figure 9. As it can be seen in this figure, an increased number of lining joints is associated with lower costs of segmental lining design and implementation since the number of joints increases, the imposed bending moment reduces, and the imposed axial forces rise. However, as the rate of reduction in the bending moment is higher than the rate of increase in the axial forces, the bending moment has a more sensible role in the decline of the cost function.

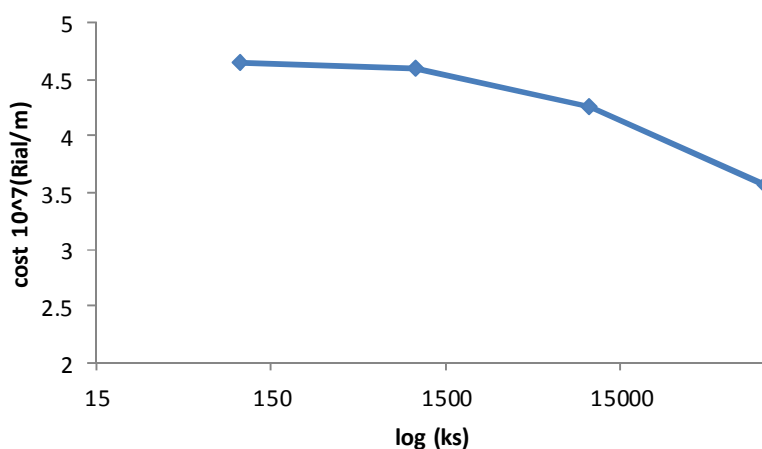


**Figure 7. Effect of soil resistance coefficient on objective function.**

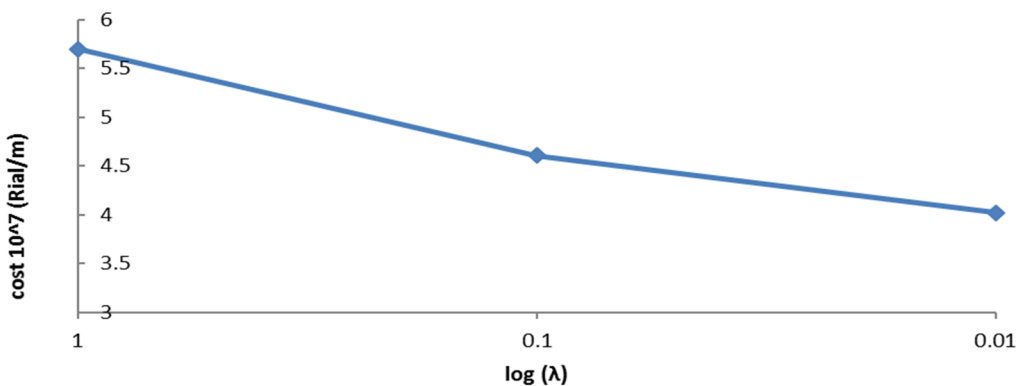


**Figure 8. Effect of joint flexural stiffness on objective function.**

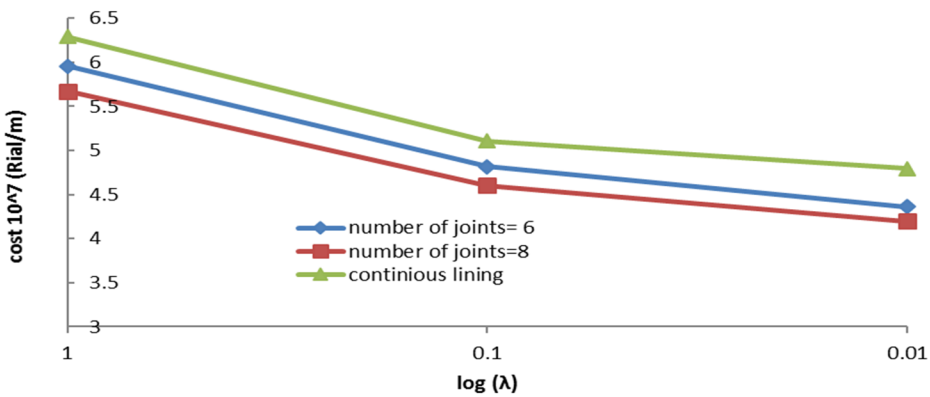


Figure 9. Effect of number of lining joints on objective function changes.

Effect of joint arrangement patterns on the objective function is demonstrated in Figure 10. As observed earlier, from a structural viewpoint, behavior of the segmental lining could be considered optimal if the first joint is located near the crown of the tunnel since the bending moment decreases under such circumstances. Accordingly, the imposed internal forces and cost of segmental lining implementation would decline in a parallel fashion.

Figure 11 shows the effect of joint arrangement patterns in terms of the diameters of the tunnel on the changes in segmental lining thickness.

As shown in this figure, increased diameters of the tunnel are associated with higher segmental lining thickness, while the amount of lining thickness in the joint arrangement pattern number one is lower compared to the other arrangements since the imposed internal forces in this pattern are lower than the other patterns.

Figures 12 and 13 demonstrate the correlations between the effects of joint arrangement patterns in terms of the diameter of the tunnel on the changes in the resulting length and area of steel reinforcement in the segmental lining, respectively.

As depicted in these figures, length of the segment and area of steel reinforcements (bars, stirrups,

and bolts) at the optimal design pattern in the joint arrangement pattern number one change steeply compared to the joint arrangement pattern number two. However, the magnitude of augmentation is more sensible in the segmental lining length compared to the steel reinforcement.

Figure 14 shows the effect of excavation diameter on the optimal cost of segmental lining, which has been analyzed at the critical section. As depicted in the figure, augmented excavation diameter is associated with an increase in the cost of optimal design. However, the magnitude of these costs may rise along with a higher rate in larger diameters due to the increased dead zone load. Furthermore, larger excavation diameters are associated with increased depth of excavation and optimal cost compared to smaller excavation diameters.

Figure 15 demonstrates the effect of soil cohesion on the cost of the optimal segmental lining design. As it can be seen in this figure, the cost of optimal design and soil cohesion decline in a parallel fashion.

As shown in this figure, the rate of reduction due to shear resistance increases at higher excavation depths. Figure 16 illustrates the effect of the internal friction angle of the medium on the cost of optimal segmental lining pattern.

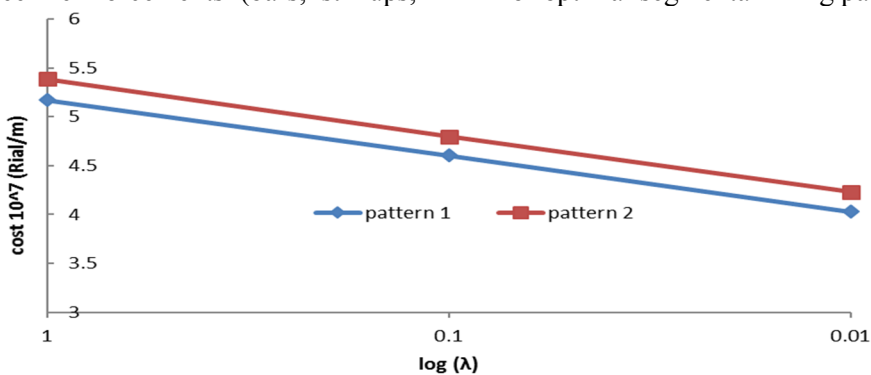


Figure 10. Effect of joint arrangement patterns on objective function.

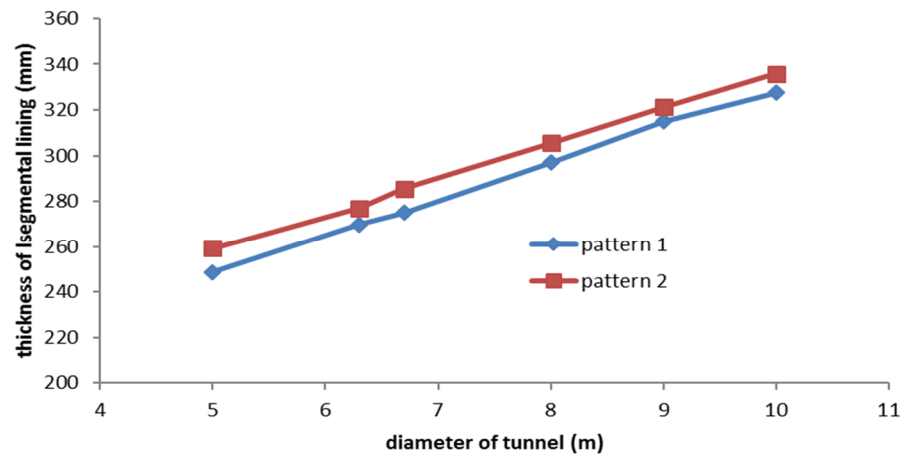


Figure 11. Effect of joint arrangement patterns on segmental lining thickness.

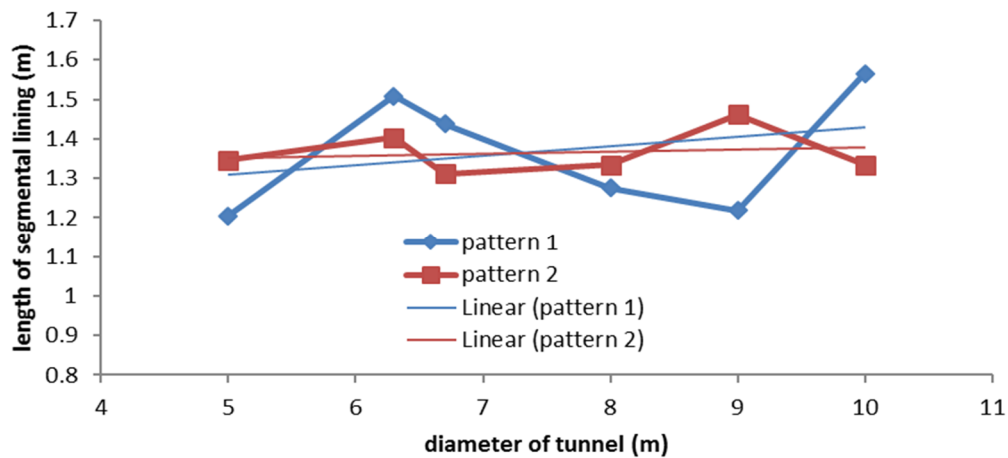


Figure 12. Effect of joint arrangement patterns on segmental lining length.

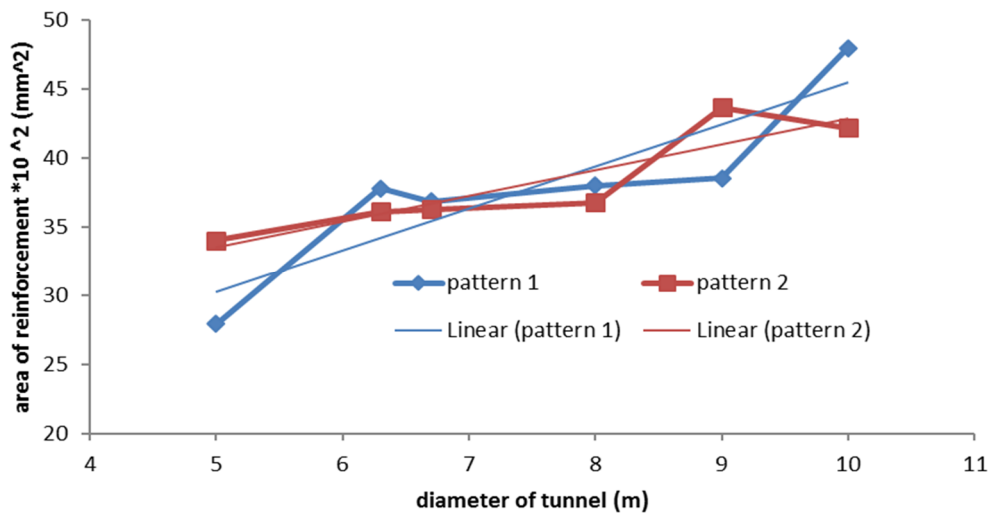
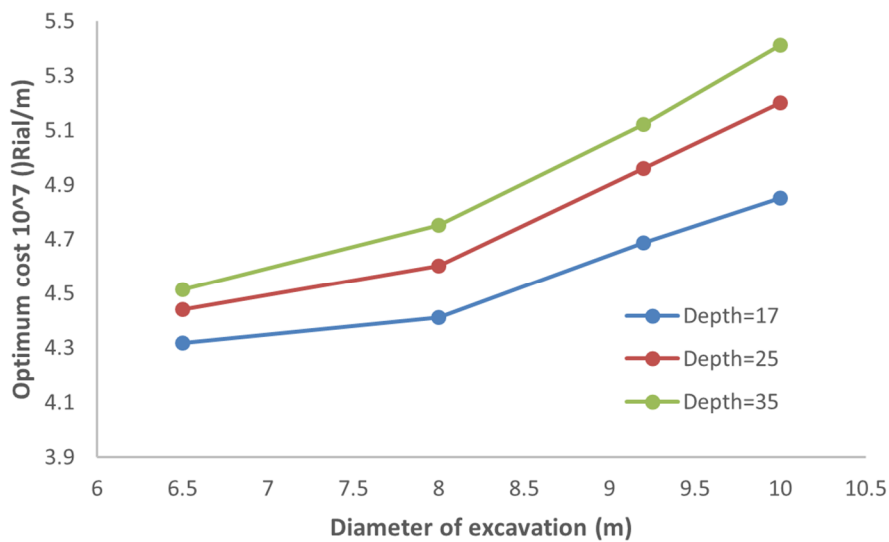
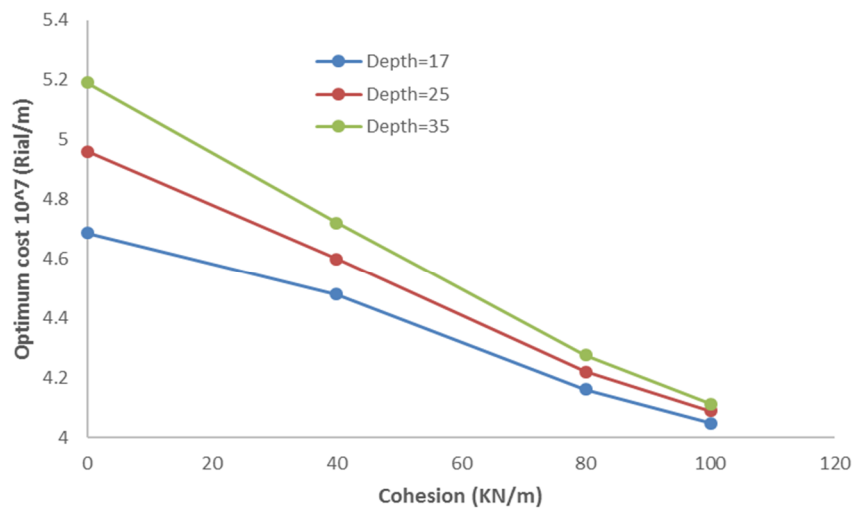


Figure 13. Effect of joint arrangement patterns on area of steel reinforcement.



**Figure 14.** Effect of excavation diameters on optimal cost of segmental lining.



**Figure 15.** Effect of soil cohesion on optimal cost of segmental lining.

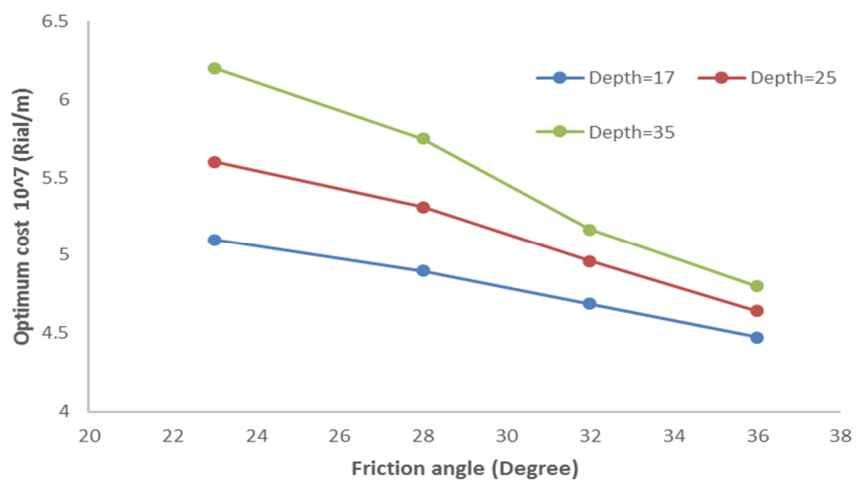


**Figure 16.** Effect of internal friction angle on optimal cost of segmental lining.

As depicted in this figure, an increased internal friction angle is associated with a reduction in the optimal cost due to higher shear resistance, by which the magnitude of reduction is more significant at higher excavation depths. Similar to soil cohesion, high rate of internal forces in the upper amount of the friction angle is less significant compared to lower values so that an increased rate of the optimal cost would have a diminishing effect on this condition.

## 5. Conclusions

The main objective of the current work was to develop a hybrid simulation-optimization model that is capable of obtaining the optimal design for reinforced concrete segmental linings in terms of cross-section dimensions and reinforcement details. Optimization was carried out using the ICA and PSO algorithms, while meeting the strength and serviceability constraints, as proposed by the American Concrete Institute and the guidelines for designing shield tunnel linings, presented by the International Tunneling Association (ITA) (Requirements for Structural Concrete and Commentary). The model was applied to the segment of Mashhad urban tunnel project as a case study to obtain its optimal design pattern, while drawing the possible conclusions and recommendations. Conclusions of this work could be summarized as what follows. The result of hybrid model revealed that the meta-heuristic algorithms had an acceptable ability to optimize the RC segmental lining as a structural tunnel support in Mechanized Tunneling. When the PSO and ICA algorithms were used as the optimization model, design and implementation costs of the RC segmental lining in Mashhad urban tunnel project were estimated at  $4.735 \times 10^7$  and  $4.6827 \times 10^7$  Rial/m in 2015, respectively, which were 12.6% and 14% lower than the cost of segmental lining ( $5.4243 \times 10^7$  Rial/m), as offered by the consulting company. With ICA as the optimization algorithm, the objective function was converged in the lower amount of iteration compared to the PSO algorithm. Moreover, the cost of optimal design using ICA was determined to be 1.5% lower than the PSO algorithm, which indicated that these algorithms would be efficient in these types of problems considering their powerful search ability in both the exploration and exploitation aspects. The results obtained showed that an increase in the number of joints augmented the flexibility of the segmental lining, thereby declining the bending moments. Consequently, an increased number of joint numbers was associated with the

decreased cost of optimal design.

## References

- [1]. Nikkhah, M., Mousavi, S.S. and Zare, Sh. (2017). Evaluation of structural analysis of tunnel segmental lining using beam-spring method and force-method (Case study: Chamshir water conveyance tunnel), Journal of Mining and Environment. 8 (1): 111-130.
- [2]. Kaveh, A. and Sabzi, O. (2011). A comparative study of two meta-heuristic algorithms for optimum designs of reinforced. International Journal of Civil Engineering. 9 (3): 193-206.
- [3]. Akin, A. and Saka, M.P. (2015). Harmony search algorithm based optimum detailed design of reinforced concrete plane frames subject to ACI 318-05 provisions. Computers and Structures. 147: 79-95.
- [4]. Camp, C.V., Pezeshk, S. and Hansson, H. (2003). Flexural design of reinforced concrete frames using a genetic algorithm. Journal of Structural Engineering. 129 (1): 105-115.
- [5]. Carbonell, A. and Gonzlez-Vidosa, F. (2011). Design of reinforced concrete road vaults by heuristic optimization. Advances in Engineering Software. 42: 151-159.
- [6]. Kaveh, A. and Ilchi Ghazaan, M. (2017). Optimum Design of Skeletal Structures Using PSO-Based Algorithms. Periodica Polytechnica Civil Engineering. 61 (2): 184-195.
- [7]. Kashania, A.R., Gandomi, A.H. and Mousavi, M. (2016). Imperialistic Competitive Algorithm: A metaheuristic algorithm for locating the critical slip surface in 2-Dimensional soil slopes. Geoscience Frontiers. 7 (1): 83-89.
- [8]. Koopialipoor, M., Fallah, A., Armaghani, D.J., Azizi, A. and Mohamad, E.T. (2018). Three hybrid intelligent models in estimating flyrock distance resulting from blasting. Engineering with Computers.
- [9]. Sahel Engineering Corporation Report. (2008). Geotechnical report of Mashhad Urban Tunnel, Line 2.
- [10]. Arthe Engineering Company Report. (2009). Structural segment design of Mashhad urban railway line 2.
- [11]. ACI 318-08m, Building Code Requirements for Structural Concrete and Commentary. (2008). American Concrete Institute (ACI).
- [12]. Wang, J.N. (1993). Seismic Design of Tunnels- A Simple State-of-the-Art Design Approach. William Barclay Parsons Fellowship, Monograph 7.
- [13]. Penzien, J. (2000). Seismically Induced Racking of Tunnel Linings. Earthquake Engineering & Structural Dynamics. 29 (5): 683-691.
- [14]. Maher Jahjouh, M. (2012). Design optimization of reinforced concrete frames using Artificial Bees

Colony Alghorithm, Master thesis of Structural Engineering, The Islamic University, Gaza.

[15]. Kennedy, J. and Eberhart, R. (1995). Particle swarm optimization, IEEE international conference on neural networks, Piscataway. pp. 1942-1948.

[16]. Kennedy, J. and Eberhart, R. (2001). Swarm Intelligence, Academic Press.1<sup>st</sup> ed, San diego, CA.

[17]. Kaveh, A. (2014). Advances in metaheuristic algorithms for optimal design of structures. Switzerland: Springer.

[18]. El-Henawy, I. and Abledmegeed, N.A. (2018).

Meta-Heuristics Algorithms: A Survey. International Journal of Computer Applications. 179 (22): 45-54.

[19]. Atashpaz-Gargari, E. and Lucas, C. (2007). Imperialist competitive algorithm: an algorithm for optimization inspired by imperialistic competition, in: CEC IEEE Congress on Evolutionary Computation.

[20]. Lee, K.M., Hou, X.Y., Ge, X.W. and Tang, Y. (2001). An Analytical Solution for A Jointed Shield-Driven Tunnel Lining. International Journal for Numerical and Analytical Geomechanics. 25 (4): 365-390.

## بررسی مقایسه‌ای دو الگوریتم فرا ابتکاری در بهینه‌سازی هزینه‌های قطعات پوشش بتنی

سید سعید موسوی، مجید نیکخواه\* و شکرالله زارع

دانشکده مهندسی معدن، نفت و ژئوفیزیک، دانشگاه صنعتی شهرورد، ایران

ارسال ۲۰۱۸/۶/۱۲، پذیرش ۲۰۱۸/۱۱/۵

\* نویسنده مسئول مکاتبات: m.nikkhah@shahroodut.ac.ir

### چکیده:

در این پژوهش روشی برای بهینه‌سازی خودکار هزینه سگمنت پوشش بتنی سیستم نگهداری در مطالعه موردی قطار شهری خط دو مشهد ارائه شده است. در این راستا دو روش فرا ابتکاری بهینه‌سازی ازدحام ذرات (PSO) و الگوریتم رقابت استعماری (ICA) استفاده شده است. تابع پنالتی برای راه حل‌های غیرقابل قبول استفاده شده و مجموع تمام جریمه‌های قیود اعمال شده می‌باشد. ۹- متغیر طراحی پوشش بتنی شامل: ۱- عرض سگمنت، ۲- ضخامت سگمنت، ۳- تعداد آرماتورهای کششی، ۴- تعداد آرماتورهای فشاری، ۵- قطر آرماتورهای کششی، ۶- قطر آرماتورهای فشاری، ۷- قطر خاموت مورد استفاده، ۸- قطر بولت اتصال دهنده سگمنت‌ها و ۹- تعداد بولتهای اتصال دهنده سگمنت‌ها در نظر گرفته شده است. همچنین، قیود طراحی طبق آیین‌نامه بتون آمریکا (ACI318M-08) و راهنمای طراحی پوشش بتنی پیشنهادی انجمن بین‌المللی تونل پیاده‌سازی شده است. تابع هدف شامل هزینه کل تأمین و اجرای اجزاء قطعات پوشش بتنی می‌شود. طراحی بهینه با استفاده از الگوریتم‌های PSO و ICA تحلیل شده‌اند. هزینه اجرای طرح بهینه به دست آمده از الگوریتم PSO و ICA به ترتیب ۱۲/۶ و ۱۴ درصد کمتر از هزینه طرح اجرا شده در پروژه است.

**کلمات کلیدی:** بهینه‌سازی فرا ابتکاری، قطعات پوشش بتنی، بهینه‌سازی ازدحام ذرات، الگوریتم رقابت استعماری، تونل‌زنی مکانیزه.